COMMUNICATION

Check for updates

Anion binding properties of a hollow PdL-cage†

Brian J. J. Timmer [ID] and Tiddo J. Mooibroek [ID]*

The hollow [PdL][BAr^F]$_2$ complex **1** of a tetra-pyridyl (py) ligand (L) has a [Pd(py)$_4$]$^{2+}$ coordination environment. Addition of coordinating anions resulted in the formation of a neutral species with Pd(py)$_2$(anion)$_2$ coordination environment (**1**^{2A}). These species bind further to the coordinating anions in the order Cl$^-$ > N$_3^-$ > Br$^-$ > I$^-$ > AcO$^-$ with $K_a^{1:1} \leq 414$ M^{-1}. With relatively non-coordinating anions **1** remains intact and displays 1:2 binding behaviour dominated by the 1:1 stoichiometry in the order NO$_3^-$ ($\sim 10^5$ M^{-1}) » ClO$_4^-$ and BF$_4^-$ ($\sim 10^3$ M^{-1}). As evidenced by crystal structure data, DFT calculations and {^{1}H−^{19}F}-HOESY NMR with BF$_4^-$, the anions are bound by charge assisted [C−H]$^+\cdots$anion interactions.

Anion recognition chemistry has potential applications in the biochemical domain, medicine, and catalysis, and anion binders can be used to detect/extract anionic pollutants from waste streams.[1] Conceptual strategies to achieve selective anion recognition are plentiful[1] and historically have revolved around the use of metal bonding,[2] hydrogen bonding interactions,[3] or a combination thereof.[4] In recent years it has become clear that other types of interactions such as anion–π interactions,[5] halogen bonds[6] and other σ–hole interactions[7] can be used to interact with anions. It has even been reported that the weakly polarized hydrogen atoms of C–H bonds can act as hydrogen bond donors for anions, especially when several such interactions work in concert.[8] Unsurprisingly, employment of electron withdrawing groups such as a somewhat distant positive charge can reinforce these otherwise weak C–H···anion interactions.[8b,9] Molecular frameworks that preorganize hydrogen bond donors are typically flexible or more rigid podand-like architectures,[8i,10] or macrocyclic designs.[8f,11] Discrete coordination compounds where the metal acts as organizing entity (*e.g.* large molecular knots and links,[12] and pyridyl complexes[13]) have also been explored for their solution phase anion recognition

van 't Hoff Institute for Molecular Sciences, University of Amsterdam, Science Park 904, Amsterdam, 1098 XH, The Netherlands. E-mail: t.j.mooibroek@uva.nl

† Electronic supplementary information (ESI) available. See DOI: 10.1039/d1cc02663a

potential. One interesting class of compounds in this regard are the so-called 'M_2L_4 cages' where 'M' is a transition metal ion and 'L' is a ditopic ligand.[14] When M is a square-planar metal such as Pd^{2+} or Pt^{2+} and the ligand is a dipyridyl ligand of appropriate size, the resulting M_2L_4 coordination cage can bear a hollow interior suitable for hosting other molecules.[14a–c] Examples of guests include anti-cancer drugs,[15] carbohydrates,[16] and anions.[17] Interestingly, anion binding with Pd$_2L_4$ complexes can be facilitated by (charge assisted) C–H···anion interactions,[17a] and M_2L_4 complexes have been reported as selective binders for nitrate[17b] or perchlorate.[17c,17d]

We recently reported on the new type of hollow molecule **1** shown in Fig. 1a for the purpose of binding carbohydrates.[18] This hybrid-design of the type 'PdL' combines design principles from M_2L_4 coordination cages with those of potent covalent macrocyclic receptors.[19] A particularly attractive feature of the design represented by **1** is that the formation of a hollow molecule is nearly stoichiometric as opposed to the often low-yielding macrocyclizations needed to make covalent macrocycles. Indeed, the addition of Pd(BAr^F)$_2$[16b] to the parent ligand gives **1** in a stoichiometric fashion based on NMR analysis.

It was observed that when **1** binds to monosaccharides, the polarized C–H bonds of the coordinated pyridyl ligands are
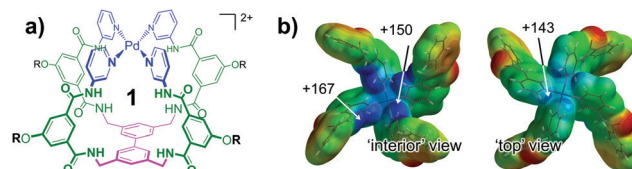

Fig. 1 (a) Coordination compound **1** studied in this work for anion recognition. R = −(CH$_2$)$_2$-*p*-Ph-C(*para*-*t*-Bu-Ph)$_3$ solubility handle and the counter anions are tetrakis(3,5-bis(trifluoromethyl)phenyl)borate (BAr^F);[18] (b) perspective views of the molecular electrostatic potential map of a fragment of **1** calculated at the DFT/ωB97X-D/6-31G* level of theory. The fragment was derived from an energy minimized structure of **1** and for clarity the 'bottom' biphenyl with four methylamides are omitted. The colour scale ranges from 41–167 kcal mol^{-1}.

typically involved in a (charge assisted) [C–H]$^+$···O hydrogen bonding interaction. This made us wonder about the anion binding properties of **1** and the possible role of charge-assisted [C–H]$^+$···anion interactions.

Particularly as the inwards facing C–H fragments are very polarized due to the dicationic nature of the [Pd(py)$_4$]$^{2+}$ complex that gives structure to the cavity. As is shown in Fig. 1b, an electrostatic potential map of a fragment of **1** indicates that the positive potential on these C–H fragments (+150 kcal mol^{-1}) is similar to that on the adjacent amidic N–H protons (+167 kcal mol^{-1}).

Binding of **1** to anions was studied by monitoring the ^{1}H-NMR resonances of **1** as a function of increasing concentration of the $^+$N(n-Bu)$_4$ salts listed in Table 1.

As is shown in Fig. 2a, addition of one equivalent of Cl$^-$ led to the disappearance of resonances that belong to the **1** with the proportional appearance of an unsymmetrical species. This is particularly evident for the resonances belonging to the inwards pointing **s3-NH** (10.5 ppm) and C–H **p2** (9.5 ppm). Both resonances are replaced by two sets of four resonances in the region 10.7–10.5 and 9.2–9.8 ppm respectively (highlighted with red lines). Addition of more Cl$^-$ caused the gradual disappearance of these eight resonances with the concomitant emergence of two sets of new resonances around 10.5 ppm in a ∼1:1.5 molar ratio. These resonances shifted about 0.4 ppm downfield upon addition of more Cl$^-$ salt, and the shifts could be fitted to a 1:1 binding model with K_a = 414 M^{-1} as listed in entry 1 of Table 1 (see also Fig. S1, ESI†). These observations are consistent with pyridyl ligand (py) displacement by one anion (forming [Pd(py)$_3$(anion)]$^+$, **1^A**) followed by a second (forming [Pd(py)$_2$(anion)$_2$], **1^{2A}**). Given that for the species **1^{2A}**, two sets of signals were observed, it is likely that these originate from *cis*- and *trans*-isomers. A similar phenomenon has been observed before with Pd$_2$L$_4$ cages, but leading exclusively to *trans*-coordinated neutral rings.[20] Species like **1^{2A}** were also obtained in the titrations with Br$^-$, I$^-$, N$_3^-$, and AcO$^-$ with accompanying affinities given in entries 2–5 of Table 1. These affinities are ordered Cl$^-$ > N$_3^-$ > Br$^-$ > I$^-$ > AcO$^-$, which is likely a reflection of the relative 'hardness'[21] of these anions.

The titrations of **1** with salts of the relatively non-coordinating NO$_3^-$,[22] ClO$_4^-$, BF$_4^-$ and PF$_6^-$ anions did not result in the formation of new species. Instead, as is illustrated

for nitrate in Fig. 2b, only peak shifting occurred. Notably, the resonance of the inwards pointing pyridinic C–H **p2** around 9.5 ppm shifted upfield to about 9.1 ppm after addition of about one equivalent of nitrate. Addition of more nitrate caused the resonance to shift an additional ∼0.1 ppm. Contrariwise, the major shift of the outwards pointing pyridinic C–H **p3** was observed after adding one equivalent of nitrate, and occurred in a downfield direction. The upfield shift of **p2** can be seen as atypical[13,22] and likely originates from displacement of interior bound DMSO, and/or a conformational change of the pyridyl rings upon binding of the nitrate (**p5** also shifted significantly).

These shifts are highly indicative of a 1:2 host (**1**) to guest (nitrate) binding stoichiometry with very strong 1:1 binding to the interior of **1** (**p2** shifts first) and weaker exterior 1:2 binding (**p3** shifts later). The shifts of **s3-NH**, **p2**, **p3**, **p5**, **b2** and **s4** were used simultaneously for curve-fitting analysis with HypNMR,[23] as is detailed in Fig. S6 (ESI†). As anticipated, straightforward fitting to a 1:1 binding model of **1** *vs* nitrate was not possible. Unexpectedly, assuming a 1:2 model did not give an accurate fit (r^2 = 0.9328). As is shown in Fig. 2c, also incorporating 2:1 binding resulted in an excellent fit to give $K_a^{2:1}$ = 36 M^{-1}, $K_a^{1:1}$ = 91.960 M^{-1} and $K_a^{1:2}$ = 2.484 M^{-1} (r^2 = 0.9976 over 168 data points). Presumably, nitrate anions can act as a bridge between two molecules of **1** by binding to the exterior of the cage. Such a 2:1 species would be present only in the very beginning of the titration, when **1** is in excess.

In the titrations with ClO$_4^-$ and BF$_4^-$ significant shifting of resonances was also observed (Fig. S7 and S8, ESI†). The resulting peak shifts could be fitted accurately to a 1:2 binding model without incorporation of the small 2:1 binding constant that was necessary in the case of nitrate. The resulting binding constants are listed in Table 1 and are about two orders of magnitude less than observed for nitrate. The weaker binding can rationalize why the 2:1 stoichiometry did not have to be incorporated in the fit for ClO$_4^-$ and BF$_4^-$. For NO$_3^-$, ClO$_4^-$ and BF$_4^-$ the 1:1 stoichiometry was significantly larger than 1:2 binding (entries 6–8 in Table 1). The 1:1 stoichiometry likely signifies binding of nitrate with the interior of **1** (*i.e.*: **p2** is shifting while **p3** is stationary), followed by 1:2 binding to the exterior of **1** (*i.e.*: **p2** is stationary while **p3** is shifting). Additional evidence for this dual binding mode was obtained in the form of a {^{1}H–^{19}F}-HOESY NMR spectrum of a sample of **1** with BF$_4^-$ (Fig. S10, ESI†). Clear intermolecular nuclear Overhauser effect (nOe) cross peaks were observed between BF$_4^-$ and the inwards pointing **s3-NH**, **p2**, and **s4**, as well as with the outwards pointing **p3**. In the titration with PF$_6^-$ (Table 1, entry 9) only relatively small shifts were observed, which could not be fitted accurately to obtain a binding constant (see Fig. S9, ESI†). Apparent, like the BAr^F anion, PF$_6^-$ does not have any specific interactions with **1**. This was confirmed by {^{1}H–^{19}F}-HOESY NMR spectroscopy of a sample of **1** containing PF$_6^-$, where no intermolecular nOe was observed (Fig. S10, ESI†).

The binding mode of NO$_3^-$, ClO$_4^-$ and BF$_4^-$ to the interior of **1** was modelled with density functional theory (DFT) calculations and (parts of) the resulting molecular models are shown in Fig. 3. In all three cases, the average C–H···O/F distance

Table 1 Overview of binding studies performed between **1** and $^+$N(n-Bu)$_4$ salts in CD$_2$Cl$_2$ with 5% DMSO-d_6

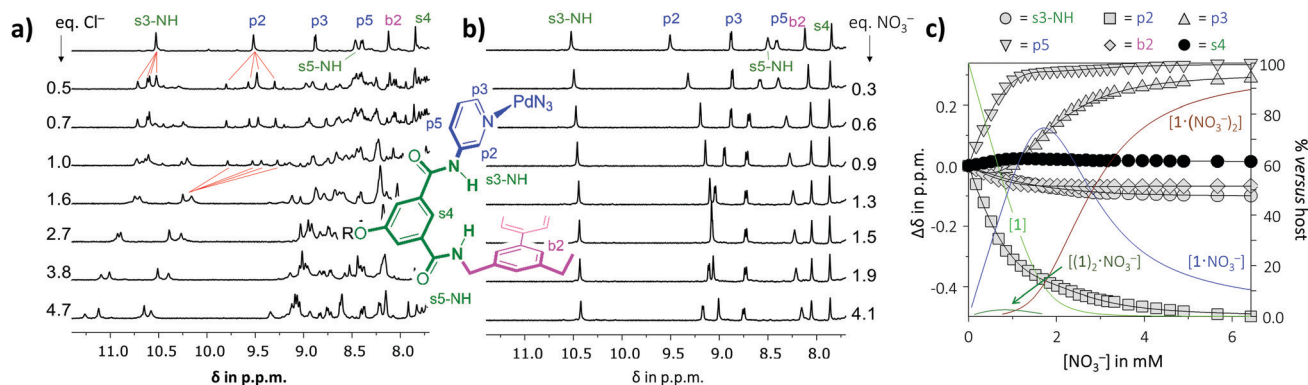| Entry	An.	K_a (M^{-1}) for **1^{2A}**	Goodness of fit (r^2)	$K_a^{1:1}$ (M^{-1}) for **1**	$K_a^{1:2}$ (M^{-1})	Goodness of fit (r^2)
1	Cl$^-$	414	0.9979	—		
2	Br$^-$	169	0.9982	—		
3	I$^-$	74	0.9942	—		
4	N$_3^-$	193	0.9887	—		
5	AcO$^-$	15	0.9777	—		
6	NO$_3^-$	—		91.960	2.484	0.9976
7	ClO$_4^-$	—		6.102	33	0.9941
8	BF$_4^-$	—		4.141	24	0.9965
9	PF$_6^-$	—		—		

Fig. 2 (a) Partial ^{1}H-NMR spectra of **1** titrated with Cl$^-$ salt. The top spectrum of **1** is assigned (see inset figure for labels) and the red lines are added as a guide to the eye. For larger scale graphic see Fig. S1 (ESI†); (b) partial ^{1}H-NMR spectra of **1** titrated with NO$_3^-$ salt. The top spectrum of **1** is assigned (see inset figure for labels and Fig. S6, ESI† for larger scale graphic); (c) HypNMR fit of peak shifting involving the indicated signals of **1** during the titration with nitrate salt. Speciation is also giving as coloured lines. Fitting to all 168 data point gave $r^2 = 0.9976$ and $K_a^{2:1} = 36$ M^{-1}; $K_a^{1:2} = 91.960$ M^{-1} and $K_a^{1:2} = 2.484$ M^{-1}. Solvent = in CD$_2$Cl$_2$ with 5% DMSO-d_6 ($^v/_v$).
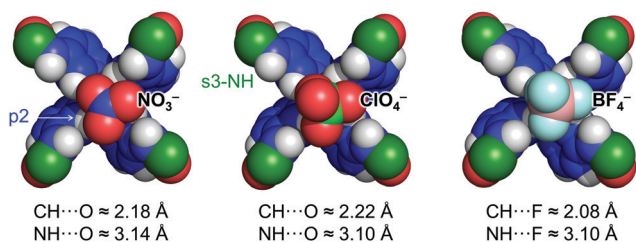

Fig. 3 Partial molecular models of **1** with internally bound NO$_3^-$, ClO$_4^-$ and BF$_4^-$ as calculated by geometry optimization at the DFT/ωB97X-D/6-31G* level of theory. The average shortest distances between the anion (O or F) and the H-atom of **p2** (CH) or **s3-NH** (NH) are listed and differ about 1 Å.

involving pyridinic C–H **p2** are about 1 Å shorter than the average N–H⋯O/F distance with the amide **s3-NH**. Actually, the average C–H⋯O/F distances are about 0.4 Å shorter than the sum of the van der Waals radii for H (1.09 Å) and O (1.52 Å) or F (1.47 Å). The average N–H⋯O/F distances on the other hand, are about 0.5 Å longer than this benchmark.

It is thus likely that interior binding of **1** for anions is established predominantly by charge-assisted [C–H]$^+$⋯anion interactions (as was also evidenced for BF$_4^-$ with HOESY NMR). Moreover, a model of [**1**·PF$_6^-$]$^+$ shown in Fig. S11 (ESI†) reveals that PF$_6^-$ barely fits inside **1** and likely experiences F⋯π
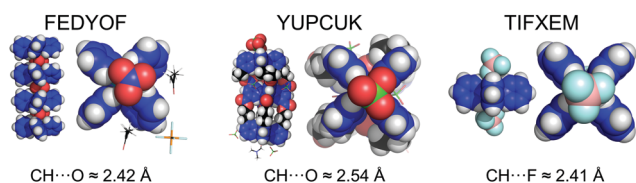

Fig. 4 Crystal structures of [Pd(py)$_4$]$^{2+}$ complexes with a nitrate (FEDYOF),[24] perchlorate (YUPCUK)[25] and tetrafluoroborate (TIFXEM)[26] anion bound to the Pd-complex with [C–H]$^+$⋯anion interactions very similar to those modelled with DFT for **1** (Fig. 3).

repulsion with the biphenyl part of **1**. This may offer a rational for the lack of binding observed with PF$_6^-$.

Finally, as is detailed in Section S5 (ESI†), a survey of the Cambridge Structure Database revealed that [C–H]$^+$⋯anion interactions involving complexes of the type [Pd(py)$_4$]$^{2+}$ are rather common. The survey also indicated a clear preference of such interactions in the order NO$_3^-$ > ClO$_4^-$ ≈ BF$_4^-$ » PF$_6^-$, which is consistent with the observed order in 1:1 binding affinities (Table 1). Three concrete examples of crystal structures with NO$_3^-$ (FEDYOF),[24] ClO$_4^-$ (YUPCUK),[25] and BF$_4^-$ (TIFXEM)[26] are shown in Fig. 4. In each case, the anion is situated very similarly as observed in the models obtained by DFT (Fig. 3) and short C–H⋯O/F distances are present. Interestingly, in the di-acetone solvate complex [Pd(pyridine)$_4$][NO$_3$][PF$_6$] FEDYOF, the PF$_6^-$ anions are not located near Pd, which implies that [Pd(py)$_4$]$^{2+}$ complexes are selective for nitrate over PF$_6^-$ in the solid state. This is consistent with the strong binding of **1** observed for NO$_3^-$ and the absence of binding for PF$_6^-$. Moreover, the nitrate anions act as a bridge in between [Pd(pyridine)$_4$]$^{2+}$ complexes to form an infinite one dimensional chain in the crystal structure. This can be seen as evidence for the feasibility of a 1:2 stoichiometry in solution. The observed bridging function of nitrate also lends further credence to the 2:1 stoichiometry that was needed to accurately fit the titration data with NO$_3^-$ (Fig. 2c). The dual binding mode to a [Pd(pyridine)$_4$]$^{2+}$ complex was also observed in TIFXEM with BF$_4^-$, but the anion does not bridge two [Pd(pyridine)$_4$]$^{2+}$ complexes. This is in line with the model used to fit the titration data with BF$_4^-$ to a 1:2 model without the use of a 2:1 stoichiometry.

In summary, Pd-complex **1** reacts with coordinating anions to eventually form charge neutral species with a Pd(py)$_2$(anion)$_2$ coordination environment (**1^{2A}**). These species bind further to the coordinating anions in the order Cl$^-$ > N$_3^-$ > Br$^-$ > I$^-$ > AcO$^-$ with a 1:1 binding stoichiometry and affinities below 10^3 M^{-1}.

With relatively non-coordinating anions, complex **1** remains intact and displays clear binding in the order NO$_3^-$ ($\sim$10^5 M^{-1}) » ClO$_4^-$ and BF$_4^-$ ($\sim$10^3 M^{-1}), while no binding was observed for PF$_6^-$. The dominant binding stoichiometry is 1:1, which is

likely binding to the interior of **1**. For NO_3^-, ClO_4^- and BF_4^-, a weaker 1 : 2 stoichiometry was also observed, while for NO_3^- an additional and very weak 2 : 1 stoichiometry had to be included in the fit. {^{1}H–^{19}F}-HOESY NMR of a sample of **1** and BF_4^- confirmed the 1 : 2 binding mode of **1**. Several crystal structures also support such 1 : 2 geometries as well as the 2 : 1 stoichiometry for a nitrate anion bridging two $[Pd(py)_4]^{2+}$ complexes. The crystal structure data, as well as DFT calculation of **1** further evidence that NO_3^-, ClO_4^- and BF_4^- anions are bound to $[Pd(py)_4]^{2+}$ complexes by charge assisted $[C–H]^+ \cdots$ anion interactions. We conclude that **1** is highly selective for nitrate, but likely too labile for actual application purposes. Adjustments of the parent ligand of **1** (*e.g.* to a di-picolinic acid derivative) in conjunction with the employment of octahedral metals might result in such more stable neutral species.

BJJT conducted the experimental work and helped write the paper. TJM wrote the paper and directed the study.

Conflicts of interest

There are no conflicts to declare.

Notes and references

1 P. D. Beer and P. A. Gale, *Angew. Chem., Int. Ed.*, 2001, **40**, 486–516.
2 (*a*) B. J. Holliday and C. A. Mirkin, *Angew. Chem., Int. Ed.*, 2001, **40**, 2022–2043; (*b*) E. J. O'Neil and B. D. Smith, *Coord. Chem. Rev.*, 2006, **250**, 3068–3080.
3 (*a*) V. Amendola, L. Fabbrizzi and L. Mosca, *Chem. Soc. Rev.*, 2010, **39**, 3889–3915; (*b*) K. Kavallieratos, C. M. Bertao and R. H. Crabtree, *J. Org. Chem.*, 1999, **64**, 1675–1683.
4 D. J. Mercer and S. J. Loeb, *Chem. Soc. Rev.*, 2010, **39**, 3612–3620.
5 (*a*) M. Staffilani, K. S. B. Hancock, J. W. Steed, K. T. Holman, J. L. Atwood, R. K. Juneja and R. S. Burkhalter, *J. Am. Chem. Soc.*, 1997, **119**, 6324–6335; (*b*) D. X. Wang and M. X. Wang, *J. Am. Chem. Soc.*, 2013, **135**, 892–897; (*c*) B. L. Schottel, H. T. Chifotides and K. R. Dunbar, *Chem. Soc. Rev.*, 2008, **37**, 68–83; (*d*) A. Frontera, P. Gamez, M. Mascal, T. J. Mooibroek and J. Reedijk, *Angew. Chem., Int. Ed.*, 2011, **50**, 9564–9583; (*e*) H. T. Chifotides and K. R. Dunbar, *Acc. Chem. Res.*, 2013, **46**, 894–906; (*f*) A. Bauza, T. J. Mooibroek and A. Frontera, *CrystEngComm*, 2016, **18**, 10–23.
6 (*a*) G. Cavallo, P. Metrangolo, T. Pilati, G. Resnati, M. Sansotera and G. Terraneo, *Chem. Soc. Rev.*, 2010, **39**, 3772–3783; (*b*) M. J. Langton, S. W. Robinson, I. Marques, V. Felix and P. D. Beer, *Nat. Chem.*, 2014, **6**, 1039–1043.
7 (*a*) A. Bauza, T. J. Mooibroek and A. Frontera, *ChemPhysChem*, 2015, **16**, 2496–2517; (*b*) P. Politzer, J. S. Murray and T. Clark, *Phys. Chem. Chem. Phys.*, 2013, **15**, 11178–11189; (*c*) S. Benz, M. Macchione, Q. Verolet, J. Mareda, N. Sakai and S. Matile, *J. Am. Chem. Soc.*, 2016, **138**, 9093–9096.
8 (*a*) M. Nishio, *Phys. Chem. Chem. Phys.*, 2011, **13**, 13873–13900; (*b*) J. J. Cai and J. L. Sessler, *Chem. Soc. Rev.*, 2014, **43**, 6198–6213; (*c*) Y. Choi, T. Kim, S. Jang and J. Kang, *New J. Chem.*, 2016, **40**, 794–802; (*d*) H. W. Wu, Y. Y. Chen, C. H. Rao and C. X. Liu, *Prog. Chem.*, 2016, **28**, 1501–1514; (*e*) Y. X. Yuan, N. N. Wu, Y. F. Han, X. Z. Song and H. B. Wang, *J. Cent. South Univ.*, 2016, **23**, 1023–1031; (*f*) Y. J. Li and A. H. Flood, *Angew. Chem., Int. Ed.*, 2008, **47**, 2649–2652; (*g*) P. Molina, F. Zapata and A. Caballero, *Chem. Rev.*, 2017, **117**, 9907–9972; (*h*) T. S. Pandian and J. Kang, *Tetrahedron Lett.*, 2015, **56**, 4191–4194; (*i*) M. Lisbjerg, H. Valkenier, B. M. Jessen, H. Al-Kerdi, A. P. Davis and M. Pittelkow, *J. Am. Chem. Soc.*, 2015, **137**, 4948–4951.
9 B. W. Tresca, R. J. Hansen, C. V. Chau, B. P. Hay, L. N. Zakharov, M. M. Haley and D. W. Johnson, *J. Am. Chem. Soc.*, 2015, **137**, 14959–14967.
10 (*a*) P. R. Brotherhood and A. P. Davis, *Chem. Soc. Rev.*, 2010, **39**, 3633–3647; (*b*) J. A. Cooper, S. T. G. Street and A. P. Davis, *Angew. Chem., Int. Ed.*, 2014, **53**, 5609–5613; (*c*) H. Y. Li, H. Valkenier, L. W. Judd, P. R. Brotherhood, S. Hussain, J. A. Cooper, O. Jurcek, H. A. Sparkes, D. N. Sheppard and A. P. Davis, *Nat. Chem.*, 2016, **8**, 24–32.
11 (*a*) M. J. Chmielewski and J. Jurczak, *Chem. – Eur. J.*, 2005, **11**, 6080–6094; (*b*) K. H. Choi and A. D. Hamilton, *Coord. Chem. Rev.*, 2003, **240**, 101–110.
12 J. F. Ayme, J. E. Beves, C. J. Campbell, G. Gil-Ramirez, D. A. Leigh and A. J. Stephens, *J. Am. Chem. Soc.*, 2015, **137**, 9812–9815.
13 (*a*) C. R. Bondy, P. A. Gale and S. J. Loeb, *Chem. Commun.*, 2001, 729–730, DOI: 10.1039/b101440o; (*b*) C. R. Bondy, P. A. Gale and S. J. Loeb, *J. Supramol. Chem.*, 2002, **2**, 93–96; (*c*) C. R. Bondy, P. A. Gale and S. J. Loeb, *J. Am. Chem. Soc.*, 2004, **126**, 5030–5031.
14 (*a*) M. Han, D. M. Engelhard and G. H. Clever, *Chem. Soc. Rev.*, 2014, **43**, 1848–1860; (*b*) A. Schmidt, A. Casini and F. E. Kuhn, *Coord. Chem. Rev.*, 2014, **275**, 19–36; (*c*) F. J. Rizzuto, L. K. S. von Krbek and J. R. Nitschke, *Nat. Rev. Chem.*, 2019, **3**, 204–222; (*d*) V. Marti-Centelles, R. L. Spicer and P. J. Lusby, *Chem. Sci.*, 2020, **11**, 3236–3240.
15 (*a*) C. Y. Zhu, M. Pan and C. Y. Su, *Isr. J. Chem.*, 2019, **59**, 209–219; (*b*) F. Kaiser, A. Schmidt, W. Heydenreuter, P. J. Altmann, A. Casini, S. A. Sieber and F. E. Kuhn, *Eur. J. Inorg. Chem.*, 2016, 5189–5196, DOI: 10.1002/ejic.201600811; (*c*) A. Schmidt, V. Molano, M. Hollering, A. Pothig, A. Casini and F. E. Kuhn, *Chem. – Eur. J.*, 2016, **22**, 2253–2256.
16 (*a*) M. Yamashina, M. Akita, T. Hasegawa, S. Hayashi and M. Yoshizawa, *Sci. Adv.*, 2017, **3**, 6; (*b*) X. Schaapkens, E. O. Bobylev, J. N. H. Reek and T. J. Mooibroek, *Org. Biomol. Chem.*, 2020, **18**, 4734–4738; (*c*) X. Schaapkens, E. O. Bobylev, J. H. Holdener, J. Tolboom, J. N. H. Reek and T. J. Mooibroek, *ChemPhysChem*, 2021, **22**, 1187–1192.
17 (*a*) T. Y. Kim, N. T. Lucas and J. D. Crowley, *Supramol. Chem.*, 2015, **27**, 734–745; (*b*) L. P. Zhou and Q. F. Sun, *Chem. Commun.*, 2015, **51**, 16767–16770; (*c*) E. Sone, M. Sato, M. Mochizuki, C. Kamio, K. Yamanishi and M. Kondo, *CrystEngComm*, 2016, **18**, 5004–5011; (*d*) P. J. Steel and D. A. McMorran, *Chem. – Asian J.*, 2019, **14**, 1098–1101; (*e*) C. Y. Fu, Y. Q. Li, L. Chen, Y. G. Wang and L. R. Lin, *Inorg. Chim. Acta*, 2019, **495**, 10.
18 B. J. J. Timmer, A. Kooijman, A. Schaapkens and T. J. Mooibroek, *Angew. Chem., Int. Ed.*, 2021, **60**, 11168–11172.
19 (*a*) T. J. Mooibroek, M. P. Crump and A. P. Davis, *Org. Biomol. Chem.*, 2016, **14**, 1930–1933; (*b*) P. Rios, T. J. Mooibroek, T. S. Carter, C. Williams, M. R. Wilson, M. P. Crump and A. P. Davis, *Chem. Sci.*, 2017, **8**, 4056–4061; (*c*) O. Francesconi, M. Martinucci, L. Badii, C. Nativi and S. Roelens, *Chem. – Eur. J.*, 2018, **24**, 6828–6836; (*d*) P. Stewart, C. M. Renney, T. J. Mooibroek, S. Ferheen and A. P. Davis, *Chem. Commun.*, 2018, **54**, 8649–8652; (*e*) O. Francesconi and S. Roelens, *ChemBioChem*, 2019, **20**, 1329–1346; (*f*) R. A. Tromans, T. S. Carter, L. Chabanne, M. P. Crump, H. Y. Li, J. V. Matlock, M. G. Orchard and A. P. Davis, *Nat. Chem.*, 2019, **11**, 52–56; (*g*) A. P. Davis, *Chem. Soc. Rev.*, 2020, **49**, 2531–2545; (*h*) O. Francesconi, F. Milanesi, C. Nativi and S. Roelens, *Angew. Chem., Int. Ed.*, 2021, **60**, 11168–11172.
20 (*a*) R. M. Zhu, J. Lubben, B. Dittrich and G. H. Clever, *Angew. Chem., Int. Ed.*, 2015, **54**, 2796–2800; (*b*) D. Preston, A. Fox-Charles, W. K. C. Lo and J. D. Crowley, *Chem. Commun.*, 2015, **51**, 9042–9045.
21 (*a*) T. L. Ho, *Chem. Rev.*, 1975, **75**, 1–20; (*b*) P. K. Chattaraj, H. Lee and R. G. Parr, *J. Am. Chem. Soc.*, 1991, **113**, 1855–1856.
22 (*a*) W. M. Bloch, J. J. Holstein, B. Dittrich, W. Hiller and G. H. Clever, *Angew. Chem., Int. Ed.*, 2018, **57**, 5534–5538; (*b*) R. Sekiya, M. Fukuda and R. Kuroda, *J. Am. Chem. Soc.*, 2012, **134**, 10987–10997.
23 C. Frassineti, S. Ghelli, P. Gans, A. Sabatini, M. S. Moruzzi and A. Vacca, *Anal. Biochem.*, 1995, **231**, 374–382.
24 U. Siriwardane and F. Fronczek, *CSD Communication*, 2017, CCDC deposition Nr 1562063.
25 G. Sarada, A. Kim, D. Kim and O. S. Jung, *Dalton Trans.*, 2020, **49**, 6183–6190.
26 A. De Leon, J. Pons, X. Solans and M. Font-Bardia, *Acta Crystallogr., Sect. E: Struct. Rep. Online*, 2007, **63**, M2164–U1264.